Desalination and Water Treatment
www.deswater.com

doi: 10.1080/19443994.2015.1040465

57 (2016) 10767–10775
May

Taylor & Francis
Taylor & Francis Group

Adsorptive removal of Cr(VI) from aqueous solutions with an effective adsorbent: cross-linked chitosan/montmorillonite nanocomposites in the presence of hydroxy-aluminum oligomeric cations

Yu-Mei Wang, Lian Duan*, Yue Sun, Ning Hu, Jin-Yun Gao, Hong Wang, Xian-Mei Xie*

School of Chemistry and Chemical Engineering, Research Institute of Special Chemicals, Taiyuan University of Technology, Taiyuan 030024, China, Tel. +86 18935128026; email: wangyumeijia90@163.com (Y.-M. Wang), Tel. +86 351 6018564; emails: duanlian@tyut.edu.cn (L. Duan), sunyue@tyut.edu.cn (Y. Sun), Tel. +86 18234085967; email: huning_syit@126.com (N. Hu), Tel. +86 15536013341; email: 15536013341@163.com (J.-Y. Gao), Tel. +86 18334707121; email: 18334707121@163.com (H. Wang), Tel. +86 351 6018564; email: xxmsxty@sina.com (X.-M. Xie)

Received 9 October 2014; Accepted 5 April 2015

ABSTRACT

On the basis of laboratory research, the adsorbent of cross-linked chitosan/Al_{13}-pillared montmorillonite (CCPM) was examined on the removal of Cr(VI) from aqueous solutions. In order to determine the effects of process parameters namely cross-linked chitosan-to-clay ratio, temperature, initial solution pH, initial Cr(VI) concentration, adsorbent dose, and contact time on Cr(VI) uptake, batch studies were systematically conducted. Equilibrium data were applied to the Langmuir and Freundlich isotherm models and best described by the Langmuir isotherm model. It was shown that monolayer adsorption capacity was 15.67 mg/g of Cr(VI) obtained by the Langmuir isotherm model. The kinetics of adsorption correlated well with the pseudo-second-order equation. Moreover, the intra-particle diffusion model was applied to investigate the mechanism of adsorption. Furthermore, thermodynamic parameters including free energy change, enthalpy change, and entropy change revealed that the adsorption of Cr(VI) onto CCPM was endothermic and spontaneous. The results suggest that CCPM is an effective adsorbent for removing Cr(VI) ions from aqueous solutions.

Keywords: Adsorption; Cr(VI); Cross-linked chitosan; Al_{13}-pillared montmorillonite; Equilibrium isotherms; Kinetics

1. Introduction

Cr(VI) is highly hazardous produced by several industries, namely leather tanning, wood preservative industries and manufacturing of dye, paper, and paint. Chromium exists in the environment in the trivalent state, that is, in the cationic form as Cr(III), or in the hexavalent state as the Cr(VI) anions: $HCrO_4^-$, CrO_4^{2-}, and $Cr_2O_7^{2-}$ [1]. If Cr(VI) enters the gastric system, it will cause some diseases: epigastric nausea, vomiting, severe diarrhea, corrosion of skin, respiratory tract, and lungs carcinoma [2]. In terms of industries, the discharge limit of Cr(VI) is less than 0.1 mg/L, while the permissible limit is 0.05 mg/L for

*Corresponding authors.

drinking water [3]. Given the protection of public health and requirement on the discharge limits, it is of vital importance to reduce any excess amount of Cr(VI) present in wastewater. The most commonly used techniques for the removal of Cr(VI) focus on methods including chemical precipitation, adsorption, electrodepositing, filtration, and membrane systems [4]. Among all of these, adsorption is now recognized as a simple and efficient method for water decontamination and separation for analytical purposes [5].

Chitosan, which contains hydroxyl (–OH) groups and amino ($–NH_2$) groups, has the ability to form complexes with metals. However, the applications of chitosan are limited because it easily dissolves in dilute organic acids and forms a gel in aqueous solution, which results in the inaccessibility of its binding sites [6]. Therefore, chemical modifications such as cross-linking step are needed to improve the chemical stability of the biosorbent in acid solutions. Montmorillonite (MMT), a low-cost adsorbent, has a crystalline structure with an alumina octahedral between two tetrahedral layers of silica. It is addressed by the modification through intercalating large organic or inorganic cations into their interlayer space. Moreover, for the preparation of Al-pillared MMT (PM), one of the most intensively studied is the hydroxy-aluminum polycations [7].

Though the scientific literature is replete with studies on preparation for chitosan/MMT composites, the chitosan/MMT nanocomposite in most studies was prepared by coating a thin layer of chitosan onto the MMT surface. Cross-linked chitosan/Al_{13}-pillared montmorillonite (CCPM), an efficient adsorbent, has been demonstrated that chitosan did enter the silicate layers by XRD and successfully used to removal Cu (II) and Pb(II) [8]. The aim of the present study was to further investigate the adsorptive features of CCPM for removing Cr(VI), considering that it may be different from removing metal cations by CCPM. The effects of the process parameters such as cross-linked chitosan-to-clay ratio, concentrations, initial pH, contact time, and adsorption temperature on Cr(VI) removal were investigated under static conditions. Finally, the applicable isotherm model, the suitable kinetic mechanism, and the thermodynamic parameters were also analyzed.

2. Experimental

2.1. Chemicals and equipment

The procedure for the preparation of the cross-linked chitosan/Al-pillared montmorillonite nanocomposite (CCPM) was the same as that reported [8]. Sodium montmorillonite (Na–Mt, 95%) was supplied by Zhejiang Sanding Technology Co., Ltd., China. Chitosan, with a deacetylation of 80.0–95.0% and average molecular weight of 9012-76-4, was supplied by Aldrich. All reagents used in this study were of analytical reagent grade. Deionized water was prepared in all experimental solutions. A UV–visible spectrophotometer colorimetrically (UV-1800, KYOTO JAPAN) was utilized at 540 nm in the analysis of residual Cr(VI). The surface area analysis of chitosan, MMT, PM, and CCPM was performed using BET-N_2 adsorption at 77 K in a Micromeritics ASAP (2020) equipment.

2.2. Solutions

A stock solution with a concentration of 1,000 mg/L of Cr(VI) was prepared by dissolving $K_2Cr_2O_7$ (2.8286 g) in a separate 1,000 mL of distilled water. The desired concentrations of experimental solutions were obtained by diluting the stock Cr(VI) standard solution with distilled water when necessary.

2.3. Batch study

Experiments were carried out using 0.5 g of CCPM and 20 mL of Cr(VI) solution on a temperature-controlled incubator shaker (150 rpm). The effects of cross-linked chitosan-to-clay ratios (0.20:1, 0.30:1, 0.45:1, 0.60:1, and 1.20:1) and initial concentration (20–600 mg/L) on Cr(VI) removal were studied. The initial pH of the reaction mixture was adjusted using 1 M HCl or 1 M NaOH. The adsorption capacity and the adsorption percentage were determined as follows:

$$q_t = \frac{(C_0 - C_e)V}{m} \tag{1}$$

$$R = \frac{(C_0 - C_e)}{C_0} \times 100\% \tag{2}$$

where q_t is adsorption capacity (mg/g) and C_e is the concentration (mg/L) of Cr(VI) at time t. V is the volume of Cr(VI) solution (mL). M is the mass of the adsorbent (g) and C_0 is the initial Cr(VI) concentration (mg/L).

2.4. Batch kinetics

The kinetic studies were performed at different temperatures (288–313 K), in which 0.5 g of adsorbent was added in 20 mL of Cr(VI) solution with initial concentration of 100 mg/L. The flasks were agitated at 150 rpm for pre-determined time intervals (5–240 min).

2.5. Equilibrium studies

Batch equilibrium studies were conducted using 20 mL aliquots of Cr(VI) at different temperatures (288–313 K), where a fixed amount (0.5 g) of adsorbent was added. The initial Cr(VI) concentration was varied from 20 to 600 mg/L.

3. Results and discussion

3.1. Surface area analysis

The surface area characterization of chitosan, MMT, PM, and CCPM are shown in Table 1. Chitosan is observed to have the least specific surface area (4.6787 m^2/g) while PM has the highest surface area (217.7490 m^2/g). The composite material (CCPM) of cross-linked chitosan and Al_{13}-pillared montmorillonite (PM) resulted in a larger surface area than that of chitosan and MMT but less than that of PM. The specific surface area is in the order of PM > CCPM > MMT > chitosan. The "inferior" properties of CCPM bead are attributed to the interaction of cross-linked chitosan in between the silicate layers of MMT. Moreover, it is also due to the occurrence of agglomeration, where the MMT hydroxylated edges interacted with each other [9].

3.2. Effect of cross-linked chitosan-to-clay ratios

The effect of the ratios of glucosamine (MW = 161 g/mol) among the cross-linked chitosan to the CEC of MMT (110 mmol/100 g) on the Cr(VI) removal is exhibited in Fig. 1. As the nanocomposite adsorbent ratio increased from 0.2:1 to 1.2:1, both the removal efficiency and the adsorption capacity increased initially, and declined afterward, reaching its optimum when the ratio was 0.6:1. It can be interpreted by that the amount of intercalated chitosan was saturated, which reduced the adsorption capability of Cr(VI) [10]. We can also find that a small quantity of cross-linked chitosan which intercalates into Al-pillared montmorillonite nanocomposite can significantly improve adsorption capacity. The modified ratio (0.6: 1) was chosen as the optimum one and was applied to the following experiments.

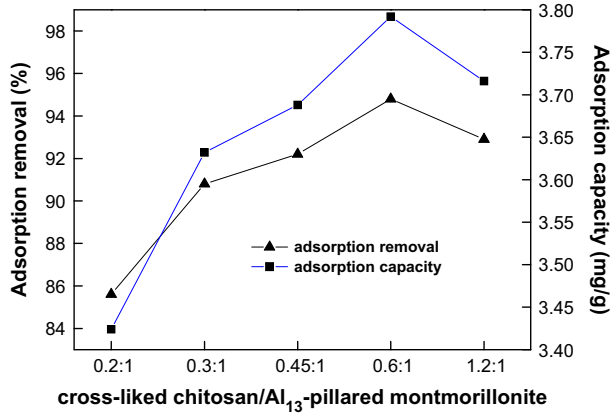

Fig. 1. Effect of modification ratio (conditions: initial concentration of Cr(VI) 100 mg/L; temperature 298 K; adsorbent dose 25 g/L; pH 5.37).

3.3. Effect of pH

Solution pH, an important factor, has a great impact on the adsorption of metal ions onto the solid–liquid interface. To determine its effect on the removal of Cr(VI), batch adsorption experiments were carried out by varying the pH range between 4.70 and 8.12 (Fig. 2). Over the pH range, the optimal uptake occurred at pH 5.37 (95%) at the given concentration. It can be observed that the adsorption onto CCPM was relatively less sensitive to an increase in pH at values lower than 7. Within the range of pH values from 7 to 8.12, the adsorption capacity declined drastically with increasing pH.

In acidic media (pH 2–6), Cr(VI) ions exist in different forms such as $Cr_2O_7^{2-}$, $HCrO_4^-$, and $HCrO_4^-$ predominates. At pH >7, chromate (CrO_4^{2-}) will preferably exist in the solution [11]. Cr(VI) uptake is higher at low pH values because most amino groups of CCPM can undergo protonation to NH_3^+ with extent of protonation, which leads to a stronger attraction for a negatively charged ion in the solution and

Table 1
Surface area determination of chitosan, MMT, PM, and CCPM adsorbent

	Chitosan	MMT	PM	CCPM
Pore volume (cm^3/g)	0.0043	0.0468	0.0497	0.0285
Average pore width (nm)	6.1983	8.6163	5.1820	6.7017
BET surface area (m^2/g)	4.6787	14.2370	217.7490	16.5747
Langmuir surface area (m^2/g)	8.7232	19.9035	289.0732	23.5284

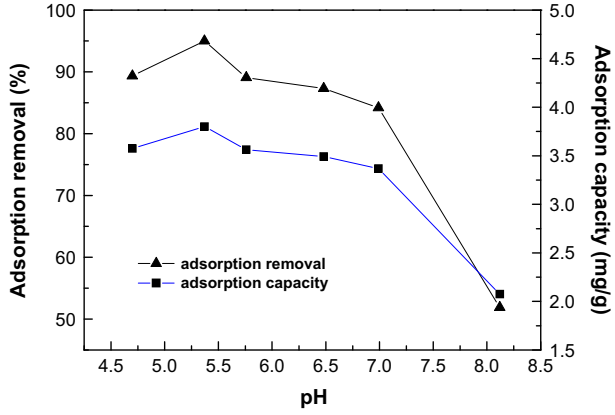

Fig. 2. Effect of pH (conditions: initial concentration of Cr(VI) 100 mg/L; temperature 298 K; adsorbent dose 25 g/L).

electrostatic interaction between the adsorbent and $HCrO_4^-$ ions [12]. As the solution pH increased, the chromate species (CrO_4^{2-}) may require more adsorption sites. Also, the competition of OH^- for the limited adsorption sites became more severe at higher pH values [13].

3.4. Effect of CCPM dose

The influence of adsorbent dose on the removal of Cr(VI) ions was discussed by varying adsorbent concentration. According to the results shown in Fig. 3, the removal efficiency of Cr(VI) ions increased significantly from 34 to 95%, with adsorption concentration increasing from 5 to 25 g/L; after the critical dose (25 g/L), additional dose of CCPM does not lead to obvious changes of Cr(VI) removal. The higher adsorbent concentration may provide greater availability of exchangeable sites for adsorption, leading to the enhanced removal efficiency. However, adsorption capacity decreased at higher adsorbent concentration because of competition of the Cr(VI) ions for the adsorption sites available [14].

3.5. Effect of contact time and temperature

Temperature and the equilibrium time play critical roles for the study of adsorption during the uptake of pollutants from wastewater. Time needed to reach equilibrium, a significant parameter, predicts the efficiency and feasibility of an adsorbent when it is used for water pollution control [15]. The adsorption of Cr(VI) onto CCPM at different temperatures was investigated as a function of time to identify the equilibrium. Based on the results in Fig. 4, it was evident that the adsorption of Cr(VI) ions onto CCPM was a fast process. Complete adsorption equilibrium was reached after 120 min. Since the adsorption process is an endothermic nature, the uptake of Cr(VI) (3.71–3.85 mg/g) is enhanced as the temperature increased from 288 to 313 K. The increase of adsorption capacity corresponding to increased temperature indicated that the adsorption of Cr(VI) ions by CCPM might involve physical as well as chemical sorption [16].

3.6. Effect of initial Cr(VI) concentration

The adsorption capacity and adsorption removal were also associated with Cr(VI) initial concentration (Fig. 5). The adsorption removal decreased from 95 to 46% as the initial Cr(VI) concentration increased from 20 to 600 mg/L. This is due to the saturation of adsorbent sites with adsorbed Cr(VI), at which point further

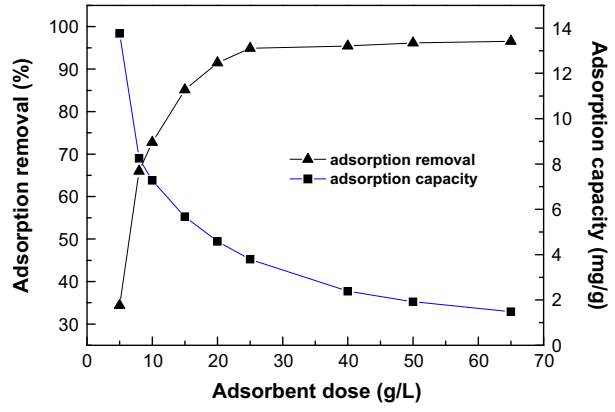

Fig. 3. Effect of adsorbent dose (conditions: initial Cr(VI) concentration 100 mg/L; volume of Cr(VI) solution 20 mL; Temperature = 298 K).

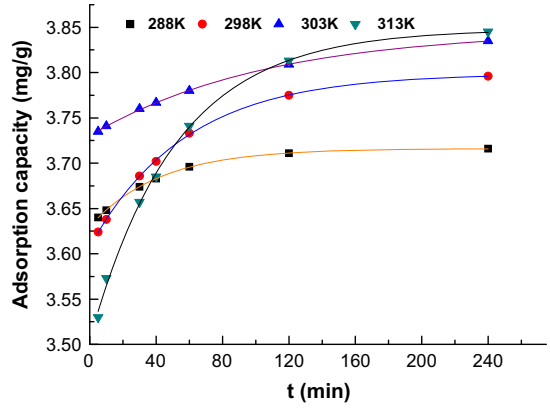

Fig. 4. Effect of temperature and contact time (conditions: initial Cr(VI) concentration 100 mg/L; pH 5.37; adsorbent dose 25 g/L).

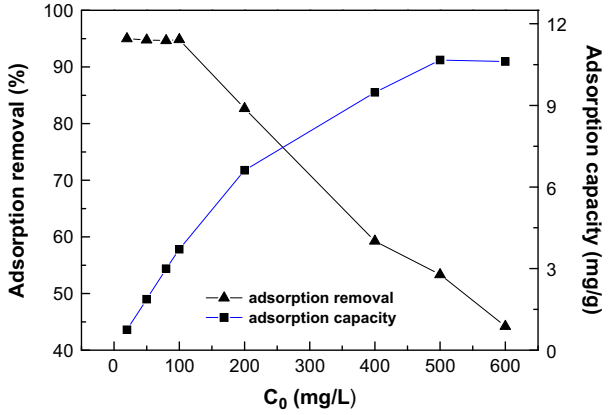

Fig. 5. Effect of initial concentration (conditions: T 298 K; pH 5.37; adsorbent dose 25 g/L).

addition of Cr(VI) hardly increases the amount of adsorbed Cr(VI) dramatically [17]. It was also observed that the adsorption capacity increased from 0.75 to 10.67 mg/g as the initial concentration increased up to 600 mg/L. This might be ascribed to the fact that driving forces of higher initial Cr(VI) concentrations can help overcome all mass transfer resistances between the aqueous solution and adsorbent surface, which leads to faster adsorption process compared to the lower concentrations of Cr(VI) at the same dose of adsorbent [18].

3.7. Adsorption isotherms

To optimize the design of an adsorption system for removing Cr(VI) from solutions, two important isotherm equations were applied to fit the equilibrium data in the present work: the Langmuir and Freundlich isotherms.

The Langmuir adsorption isotherm [19] can be described by assuming a homogeneous surface with adsorption on each equal site. Besides, the adsorption at one site does not affect adsorption at an adjacent site. The adsorption data were applied to the equation:

$$\frac{C_e}{q_e} = \frac{C_e}{Q_{max}} + \frac{1}{Q_{max} K_L} \tag{3}$$

where C_e is equilibrium concentration of Cr(VI) (mg/L), q_e is the amount absorbed by per unit mass of the adsorbent at equilibrium (mg/g), Q_{max} is the Langmuir constant that means the maximum capacity (mg/g), and the other Langmuir constant K_L which is related to the energy of adsorption (L/mg).

The values of Q_{max} and K_L can be obtained by the slope and intercept of the straight line of C_e/q_e vs. C_e.

In order to further analyze Langmuir equation, the dimensionless equilibrium parameter can be determined by:

$$R_L = \left(\frac{1}{1 + K_L C_0}\right) \tag{4}$$

where C_0 (mg/L) is the initial Cr(VI) concentration. The R_L value determines the feasibility of adsorption process. The obtained R_L values (listed in Table 1) were lying between 0 and 1, which indicated that the adsorption of Cr(VI) was favorable [16].

The Freundlich isotherm [20], an empirical equation, can be applied for adsorption onto heterogeneous surfaces and multi-molecular layer. The equation is expressed as follows:

$$q_e = K_F C_e^{1/n} \tag{5}$$

The linear form:

$$\ln q_e = \ln K_F + \frac{\ln C_e}{n} \tag{6}$$

where K_F is the Freundlich adsorption constant which is indicative of the adsorption capacity of the adsorbent (mg/g) and $1/n$ is the constant related to the intensity of the adsorption.

The values of $1/n$ and K_F were calculated from the slope and intercept by plotting ln q_e vs. ln C_e.

All the correlation coefficients, the R^2 values, and the constants obtained from the two isotherm models are listed in Table 2. On the basis of the correlation coefficients (R^2), Freundlich isotherm model failed to describe Cr(VI) adsorption on CCPM. The Langmuir

Table 2
Isotherm constants obtained for the adsorption of Cr(VI) on CCPM

Isotherm models	298 K	303 K	313 K
Langmuir			
Q_{max} (mg/g)	11.168	14.428	15.670
K_L	0.0586	0.0604	0.0679
R^2	0.9958	0.9894	0.9973
R_L	0.1457	0.1420	0.1282
Freundlich			
K_F	1.15	1.13	1.46
$1/n$	0.421	0.517	0.481
R^2	0.897	0.876	0.841

model correlated well with the equilibrium data, as given by the highest R^2 values ($R^2 > 0.98$). This implies that the adsorption process was a monolayer adsorption. Moreover, the value of Q_{max} obtained from the Langmuir model, which was 15.67 mg/g at 313 K, is approximately equal to the experimental one (14.72 mg/g). Table 3 compares the adsorption capacities and experimental conditions of chitosan composites for Cr(VI). The experimental data were well described by the Langmuir isotherm except the adsorbent chitosan/MMT and chitosan/ceramic alumina. The adsorption capacity of CCPM (15.67 mg/g) is relative higher than the adsorbent chitosan/cellulose (13.05 mg/g) with shorter equilibrium time (2 h). However, it needs 4–6 h and 5 h to reach equilibrium with higher capacity using chitosan/MMT and chitosan/perlite, respectively. Compared to the preparation of CCPM, the adsorbent magnetic chitosan was synthesized under the protection of N_2 purge gas. For the adsorbent chitosan/ceramic alumina, the experiments were carried out in bed column, which should consider a series of conditions: bed volume, number of bed volume, and flow rate. Consequently, both the material and procedure must be considered.

3.8. Adsorption kinetics

The study of adsorption kinetics was necessary, with regard to the fact that it provided valuable insight into the reaction pathways and into the mechanism of the reaction [14,15]. For this, two kinetic models including pseudo-first-order and pseudo-second-order were used.

The Lagergren's pseudo-first order, determining the rate constant of Cr(VI) adsorption, is expressed as follows [26]:

$$\ln(q_e - q_t) = \ln q_e - k_1 t \tag{7}$$

where q_t (mg/g) is the adsorption capacity at any given time (min), k_1 (1/min) is the pseudo-first-order kinetic rate constant.

The pseudo-second-order equation was based on the equilibrium adsorption, assuming that adsorption process involves chemisorption mechanism [27]. It can be described as follows:

$$\frac{t}{q_t} = \frac{1}{h} + \frac{t}{q_e} \tag{8}$$

$$h = k_2 q_e^2 \tag{9}$$

where k_2 (g/mg/min) is the equilibrium rate constant which can be calculated through plotting t/q_t against t.

Kinetic parameters were calculated and are listed in Table 4. It can be found that the k_1 values decreased with increasing temperature, which demonstrates that adsorption was faster at higher temperature. Moreover, both the higher coefficients of determination (R^2) and

Table 3
Adsorption capacities and experimental conditions of chitosan composites for Cr(VI)

Adsorbent	Type of study	Q_{max} (mg/g)	pH	Isotherm	Equilibrium time (h)	References
Chitosan/cellulose	Batch	13.05	5.8	Langmuir	10	[21]
Chitosan/MMT	Batch	41.67	4.0	Frendlich	4–6	[22]
Magnetic chitosan	Batch	69.40	4.0	Langmuir	1	[23]
Chitosan/perlite	Batch	153.8	4.0	Langmuir	5	[24]
Chitosan/Ceramic alumina	Column	153.8	4.0	Frendlich		[25]
CCPM	Batch	15.67	5.37	Langmuir	2	This study

Table 4
Kinetics parameters for Cr(VI) adsorption on CCPM

	Pseudo-first order reaction kinetics				Pseudo-second-order reaction kinetics			
T/K	R^2	k_1 (min^{-1})	$q_{e,cal}$	$q_{e,found}$	R^2	k_2 (g/(mg min))	$q_{e,cal}$	$q_{e,found}$
288	0.999	0.054	0.085	3.716	1.000	0.954	3.720	3.716
298	0.999	0.042	0.191	3.796	0.999	0.340	3.804	3.796
303	0.998	0.026	0.107	3.835	0.999	0.463	3.840	3.835

the excellent agreement between the calculated and experimental values led to the development of a conclusion in which the adsorption process follows the pseudo-second-order model.

The present data were suitable to the pseudo-second-order equation, demonstrating that chemisorption act as the rate-controlling step, which involves a sharing or exchange of electrons between the adsorbate and the adsorbent [12]. A similar phenomenon has been reported in the literature for removing Cr(VI) for the adsorbents [14,15].

The adsorption kinetics were then further analyzed to identify the rate-controlling step using the intra-particle diffusion model [28], which can be represented by the following equation:

$$q_t = k_p t^{1/2} + C \tag{10}$$

where the slope k_p (mg/g/min$^{1/2}$) is the intra-particle diffusion rate constant, and C represents the thickness of boundary layer. If the rate-limiting process was only due to the intra-particle diffusion, then these lines pass through the origin ($C = 0$) [29]. Otherwise, external mass transfer is involved to some degree.

Based on these plots (Fig. 6), the sorption processes are comprised by two phases, implying that more than one process affected the adsorption for the whole reaction [30]. At the beginning, diffusion of Cr(VI) was fast from the solution to the external surface of CCPM. Then, Cr(VI) entered into the inner of CCPM and adsorbed onto the interior adsorption sites as the external surface of the adsorbent reached saturation [29]. The two stages in the plot indicate that the adsorption process occurred by surface adsorption and intra-particle diffusion.

3.9. Thermodynamics of adsorption

In order to better understand the effect of temperature on the adsorption of Cr(VI), the thermodynamic parameters such as fee Gibbs energy (ΔG), enthalpy (ΔH), and entropy (ΔS) were studied

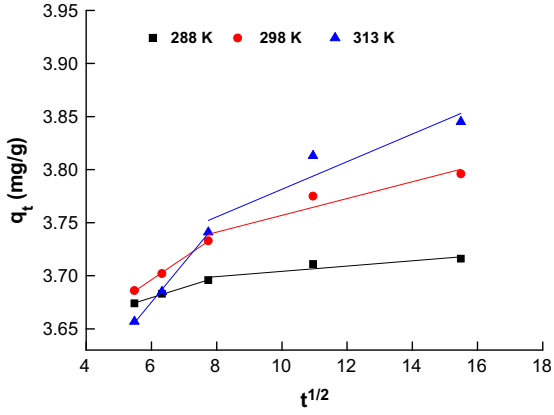

Fig. 6. Plots of intra-particle diffusion model for adsorption of Cr(VI) on CCPM.

(Table 5). The constants were computed using the following relationships:

$$K_0 = \frac{C_{ad}}{C_e} \tag{11}$$

where C_{ad} (mg/L) is the equilibrium concentration of Cr(VI) adsorbed on CCPM, and C_e (mg/L) is the equilibrium concentration of Cr(VI) in aqueous solution.

The standard free energy (ΔG) is calculated by the following equation:

$$\Delta G = -RT \ln K_0 \tag{12}$$

where T is temperature in Kelvin (273 K) and R is gas constant (8.314 J/(mol K)). Enthalpy change (ΔH) can be calculated by the relationships:

$$\Delta G = \Delta H - T\Delta S \tag{13}$$

$$\ln K_0 = \frac{\Delta S}{R} - \frac{\Delta H}{RT} \tag{14}$$

According to Eq. (14), ΔH and ΔS were obtained from the slope and intercept (Table 5). The positive ΔS was

Table 5
Thermodynamic parameters for adsorption of Cr(VI) on CCPM

T (K)	K_0	$-\Delta G$ (kJ/mol)	ΔH (kJ/mol)	ΔS (kJ/(mol K))
298	12.89	5.80		
303	13.29	5.87	40.10	0.155
313	26.78	7.46		

in line with the increased randomness appeared on the solid–solution interface during Cr(VI) adsorption process onto CCPM [31]. The value of ΔH is positive, which showed that the adsorption process was endothermic. The negative ΔG reflected that the adsorption reaction was a spontaneous and thermodynamically favorable process. Furthermore, the adsorption of Cr(VI) ions onto CCPM proceeded physically because of ΔG values were lower than −20 kJ/mol [32].

4. Conclusion

CCPM was successfully prepared as an efficient adsorbent to remove Cr(VI) ions in solution. Removal of Cr(VI) is found to be effective in the lower pH range and at higher temperatures. Equilibrium data exhibited high correlation with the Langmuir model over the overall concentration range studied. The maximum monolayer adsorption capacity Q_{max} for Cr(VI) adsorption onto CCPM was 15.67 mg/g at 313 K. Kinetic study can be best described by the pseudo-second-order equation. Moreover, as a result of intra-particle diffusion analysis, the adsorption of Cr(VI) ions onto CCPM involved intra-particle diffusion; however, that was not the only rate-controlling step. Thermodynamic parameters suggested that the adsorption was an endothermic and spontaneous process. The mechanism may include mainly ionic interactions (chemical interactions) as well as electrostatic attraction (physical interactions). The above results further demonstrated that CCPM was an effective adsorbent on the removal of Cr(VI).

Acknowledgments

This study was supported by the National Natural Science Foundation of China (grant number 21301126), the Shanxi Province Science Foundation for Youths (grant number 2013021009-3), the Industrial Research Program for Tax Problems of Shanxi Province (grant number 20130321033-02), the Science and Technology Projects of Taiyuan City (grant number 120238).

References

[1] R.H.B. Yang, Q. Liu, Y. Liu, Simultaneous adsorption of aniline and Cr(VI) ion by activated carbon/chitosan composite, J. Appl. Polym. Sci. 131 (2014) 1–9.
[2] A.C. Zimmermann, A. Mecabô, T. Fagundes, C.A. Rodrigues, Adsorption of Cr(VI) using Fe-crosslinked chitosan complex (Ch-Fe), J. Hazard. Mater. 179 (2010) 192–196.
[3] S.H. Altungodan, Cr(VI) removal from aqueous solution by iron (III) hydroxide-loaded sugar beet pulp, Process Biochem. 40 (2005) 1443–1452.
[4] H. Sufia, Removal of chromium hexavalent ion from aqueous solutions using biopolymer chitosan coated with poly 3-methyl thiophene polymer, J. Hazard. Mater. 181 (2010) 474–479.
[5] N. Sm, P. Kumaran, Removal of heavy metal from industrial wastewater using chitosan coated oil palm shell charcoal, Electron. J. Biotechnol. 8 (2005) 43–53.
[6] C.M. Futalan, C. Kan, M.L. Dalida, C. Pascua, M. Wan, Fixed-bed column studies on the removal of copper using chitosan immobilized on bentonite, Carbohydr. Polym. 83 (2011) 697–704.
[7] W. Tan, Y. Zhang, Y.S. Szeto, L. Liao, A novel method to prepare chitosan/montmorillonite nanocomposites in the presence of hydroxy-aluminum oligomeric cations, Compos. Sci. Technol. 68 (2008) 2917–2921.
[8] L. Duan, N. Hu, T. Wang, H. Wang, L. Ling, Y. Sun, X. Xie, Removal of copper and lead from aqueous solution by adsorption onto cross-linked chitosan/montmorillonite nanocomposites in the presence of hydroxyl-aluminum oligomeric cations: Equilibrium, kinetic, and thermodynamic studies, Chem. Eng. Commun. (2014), doi:10.1080/00986445.2014.956735.
[9] S.F. Wang, L. Shen, Y.J. Tong, L. Chen, I.Y. Phang, P.Q. Lim, T.X. Liu, Biopolymer chitosan/montmorillonite nanocomposites: Preparation and characterization, Polym. Degrad. Stab. 90 (2005) 123–131.
[10] Y. Wen, Z. Tang, Y. Chen, Y. Gu, Adsorption of Cr(VI) from aqueous solutions using chitosan-coated fly ash composite as biosorbent, Chem. Eng. J. 175 (2011) 110–116.
[11] Z. Wu, S. Li, J. Wan, Y. Wang, Cr(VI) adsorption on an improved synthesised cross-linked chitosan resin, J. Mol. Liq. 170 (2012) 25–29.
[12] X. Hu, J. Wang, Y. Liu, X. Li, G. Zeng, Z. Bao, X. Zeng, A. Chen, F. Long, Adsorption of chromium (VI) by ethylenediamine-modified cross-linked magnetic chitosan resin: Isotherms, kinetics and thermodynamics, J. Hazard. Mater. 185 (2011) 306–314.
[13] S. Mallick, S.S. Dash, K.M. Parida, Adsorption of hexavalent chromium on manganese nodule leached residue obtained from NH_3–SO_2 leaching, J. Colloid Interface Sci. 297 (2006) 419–425.
[14] S.S. Baral, S.N. Das, Adsorption of Cr(VI) using thermally activated weed Salvinia cucullata, Chem. Eng. J. 139 (2008) 245–255.
[15] S. Chen, Q. Yue, B. Gao, X. Xu, Equilibrium and kinetic adsorption study of the adsorptive removal of Cr(VI) using modified wheat residue, J. Colloid Interface Sci. 349 (2010) 256–264.
[16] L. Zhang, W. Xia, B. Teng, X. Liu, W. Zhang, Zirconium cross-linked chitosan composite: Preparation, characterization and application in adsorption of Cr(VI), Chem. Eng. J. 229 (2013) 1–8.
[17] J. Zhu, H. Gu, J. Guo, M. Chen, H. Wei, Z. Luo, H.A. Colorado, N. Yerra, D. Ding, Mesoporous magnetic carbon nanocomposite fabrics for highly efficient Cr(VI) removal, J. Mater. Chem. A 2 (2014) 2256–2265.
[18] E. Malkoc, Y. Nuhoglu, Potential of tea factory waste for chromium(VI) removal from aqueous solutions: Thermodynamic and kinetic studies, Sep. Purif. Technol. 54 (2007) 291–298.
[19] A.L. Ahmad, S. Sumathi, B.H. Hameed, Adsorption of residue oil from palm oil mill effluent using powder

and flake chitosan: Equilibrium and kinetic studies, Water Res. 39 (2005) 2483–2494.
[20] M.S. Chiou, H.Y. Li, Equilibrium and kinetic modeling of adsorption of reactive dye on cross-linked chitosan beads, J. Hazard. Mater. 93 (2002) 233–248.
[21] X. Sun, B. Yang, J. Chen, D. Li, Chitosan(chitin)/cellulose composite biosorbents prepared using ionic liquid for heavy metal ions adsorption, AlChE J. 55 (2009) 2062–2069.
[22] D. Fan, X. Zhu, M. Xu, J. Yan, Adsorption properties of chromium (VI) by chitosan coated montmorillonite, J. Biol. Sci. 6 (2007) 941–945.
[23] G. Huang, H. Zhang, J.X. Shi, T.A.G. Langrish, Adsorption of chromium(VI) from aqueous solutions using cross-linked magnetic chitosan beads, Ind. Eng. Chem. Res. 48 (2009) 2646–2651.
[24] S. Hasan, A. Krishnaiah, T.K. Ghosh, D.S. Viswanath, V.M. Boddu, E.D. Smith, Adsorption of chromium(VI) on chitosan-coated perlite, Sep. Sci. Technol. 38 (2003) 3775–3793.
[25] V.M. Boddu, K. Abburi, J.L. Talbott, E.D. Smith, Removal of hexavalent chromium from wastewater using a new composite chitosan biosorbent, Environ. Sci. Technol. 37 (2003) 4449–4456.
[26] M.E. Argun, S. Dursun, A new approach to modification of natural adsorbent for heavy metal adsorption, Bioresour. Technol. 99 (2008) 2516–2527.
[27] S.S. Baral, S.N. Das, P. Rath, G.R. Chaudhury, Chromium(VI) removal by calcined bauxite, Biochem. Eng. J. 34 (2007) 69–75.
[28] S. Basha, Z.V.P. Murthy, B. Jha, Sorption of Hg(II) onto carica papaya: Experimental studies and design of batch sorber, Chem. Eng. J. 147 (2009) 226–234.
[29] X. Wang, F. Liu, L. Lu, S. Yang, Y. Zhao, L. Sun, S. Wang, Individual and competitive adsorption of Cr (VI) and phosphate onto synthetic Fe–Al hydroxides, Colloids Surf., A 423 (2013) 42–49.
[30] Y.S. Ho, A.E. Ofomaja, Kinetics and thermodynamics of lead ion sorption on palm kernel fibre from aqueous solution, Process Biochem. 40 (2005) 3455–3461.
[31] P. Pal, F. Banat, Comparison of heavy metal ions removal from industrial lean amine solvent using ion exchange resins and sand coated with chitosan, J. Nat. Gas Sci. Eng. 18 (2014) 227–236.
[32] A.G. Yavuz, E. Dincturk-Atalay, A. Uygun, F. Gode, E. Aslan, A comparison study of adsorption of Cr(VI) from aqueous solutions onto alkyl-substituted polyaniline/chitosan composites, Desalination 279 (2011) 325–331.